

Journal of Visualized Experiments

Label-free optical technique for identifying lymphocyte types using 3D quantitative phase imaging and machine learning

--Manuscript Draft--

Article Type:	Methods Article - JoVE Produced Video
Manuscript Number:	JoVE58305R2
Full Title:	Label-free optical technique for identifying lymphocyte types using 3D quantitative phase imaging and machine learning
Keywords:	quantitative phase imaging; optical diffraction tomography; holotomography; holographic microscopy; lymphocyte identification; immune cell; immunology; machine learning; label-free imaging
Corresponding Author:	YongKeun Park Korea Advanced Institute of Science and Technology daeyeon, KOREA, REPUBLIC OF
Corresponding Author's Institution:	Korea Advanced Institute of Science and Technology
Corresponding Author E-Mail:	yk.park@kaist.ac.kr
Order of Authors:	Jonghee Yoon YoungJu Jo Young Seo Kim Yeongjin Yu Sumin Lee Wei Sun Park YongKeun Park
Additional Information:	
Question	Response
Please indicate whether this article will be Standard Access or Open Access.	Standard Access (US\$2,400)
Please indicate the city, state/province, and country where this article will be filmed . Please do not use abbreviations.	KAIST, 291 daehak-ro, yusung-gu, daeyeon 34141, republic of korea



July 27, 2018

Dear Editor:

We thank the Editor for processing, formatting, and editorially reviewing our submission (JoVE58305, Yoon *et al.*). After carefully studying the editorial comments, we revised the manuscript by addressing all concerns raised by the Editor. In particular, we thoroughly revised the protocol section to provide detailed experimental steps as required by the Editor.

Below we address the editorial comments and the list of changes that we have made to our manuscript according to the concerns. The original editorial comments are provided in **black**, whereas our answers are given in **blue**. We believe that these modifications have strengthened the protocol and hope that it is now suitable for publication in *Journal of Visualized Experiments*.

Sincerely,
YongKeun (Paul) Park,
On behalf of all co-authors

YongKeun (Paul) Park, Ph.D.

Associate Professor, Department of Physics, KAIST
Director, Time-reversal Mirror Creative Research Center <http://bmol.kaist.ac.kr>
Cofounder and CTO, Tomocube <http://www.tomocube.com>
Cofounder and Advisor, TheWaveTalk <http://www.thewavetalk.com>
Fellow, OSA
Phone: +82.42.350.2514

TITLE:

Label-Free Identification of Lymphocyte Subtypes using Three-Dimensional Phase Imaging and Machine Learning

AUTHORS & AFFILIATIONS:

Jonghee Yoon¹, YoungJu Jo^{2,3,4}, Young Seo Kim^{3,4,5}, Yeongjin Yu^{2,3}, Jiyeon Park⁶, Sumin Lee⁴, Wei Sun Park^{2,3}, YongKeun Park^{2,3,4}

¹Department of Physics, University of Cambridge, Cambridge, UK

²Department of Physics, Korea Advanced Institute of Science and Technology (KAIST), Daejeon, Republic of Korea

³KAIST Institute for Health Science and Technology, KAIST, Daejeon, Republic of Korea

⁴Tomocube, Inc., Daejeon, Republic of Korea

⁵Department of Chemical and Biomolecular Engineering, KAIST, Daejeon, Republic of Korea

⁶Department of Biological Sciences, KAIST, Daejeon, Republic of Korea

Corresponding Author:

YongKeun Park (yk.park@kaist.ac.kr)

Tel: +82-42-350-2514

Email Addresses of Co-authors:

Jonghee Yoon (jh.yoon@kaist.ac.kr)

YoungJu Jo (astralatom@kaist.ac.kr)

Young Seo Kim (ykim717@kaist.ac.kr)

Yeongjin Yu (u.yeongjin@kaist.ac.kr)

Jiyeon Park (kinu_jy@kaist.ac.kr)

Sumin Lee (slee@tomocube.com)

Wei Sun Park (weisunp@kaist.ac.kr)

KEYWORDS:

Quantitative phase imaging, optical diffraction tomography, holotomography, holographic microscopy, lymphocyte identification, immune cell, immunology, machine learning, label-free imaging

SUMMARY:

We describe a protocol for the label-free identification of lymphocyte subtypes using quantitative phase imaging and a machine learning algorithm. Measurements of 3D refractive index tomograms of lymphocytes present 3D morphological and biochemical information for individual cells, which is then analyzed with a machine-learning algorithm for identification of cell types.

ABSTRACT:

We describe here a protocol for the label-free identification of lymphocyte subtypes using quantitative phase imaging and machine learning. Identification of lymphocyte subtypes is important for the study of immunology as well as diagnosis and treatment of various diseases.

Currently, standard methods for classifying lymphocyte types rely on labeling specific membrane proteins via antigen-antibody reactions. However, these labeling techniques carry the potential risks of altering cellular functions. The protocol described here overcomes these challenges by exploiting intrinsic optical contrasts measured by 3D quantitative phase imaging and a machine learning algorithm. Measurement of 3D refractive index (RI) tomograms of lymphocytes provides quantitative information about 3D morphology and phenotypes of individual cells. The biophysical parameters extracted from the measured 3D RI tomograms are then quantitatively analyzed with a machine learning algorithm, enabling label-free identification of lymphocyte types at a single-cell level. We measure the 3D RI tomograms of B, CD4+ T, and CD8+ T lymphocytes and identified their cell types with over 80% accuracy. In this protocol, we describe the detailed steps for lymphocyte isolation, 3D quantitative phase imaging, and machine learning for identifying lymphocyte types.

INTRODUCTION:

Lymphocytes can be classified into various subtypes including B, helper (CD4+) T, cytotoxic (CD8+) T, and regulatory T cells. Each lymphocyte type has a different role in the adaptive immune system; for example, B lymphocytes produce antibodies, whereas T lymphocytes detect specific antigens, eliminate abnormal cells, and regulate B lymphocytes. Lymphocyte function and regulation is tightly controlled by and related to various diseases including cancers¹, autoimmune diseases², and viral infections³. Thus, the identification of lymphocyte types is important to understand their pathophysiological roles in such diseases and for immunotherapy in clinics.

Currently, methods for classifying lymphocyte types rely on antigen-antibody reactions by targeting specific surface membrane proteins or surface markers⁴. Targeting surface markers is a precise and accurate method to determine lymphocyte types. However, it requires expensive reagents and time-consuming procedures. Furthermore, it carries risks of the modification of membrane protein structures and the alteration of cellular functions.

To overcome these challenges, the protocol described here introduces the label-free identification of lymphocyte types using 3D quantitative phase imaging (QPI) and machine learning⁵. This method enables the classification of lymphocyte types at a single-cell level based on morphological information extracted from label-free 3D imaging of individual lymphocytes. Unlike conventional fluorescence microscopy techniques, QPI utilizes refractive index (RI) distributions (intrinsic optical properties of live cells and tissues) as optical contrast^{6,7}. The RI tomograms of individual lymphocytes represent phenotypic information specific to subtypes of lymphocytes. In this case, to systemically utilize 3D RI tomograms of individual lymphocytes, a supervised machine learning algorithm was utilized.

Using various QPI techniques, the 3D RI tomograms of cells have been actively used for the study of cell pathophysiology because they provide a label-free, quantitative imaging capability⁸⁻¹³. Also, the 3D RI distributions of individual cells can provide morphological, biochemical, and biomechanical information about cells. 3D RI tomograms have been previously utilized in the fields of hematology¹⁴⁻¹⁷, infectious diseases¹⁸⁻²⁰, immunology²¹, cell biology^{22,23}, inflammation²⁴, cancer²⁵, neuroscience^{26,27}, developmental biology²⁸, toxicology²⁹, and microbiology^{12,30-32}.

Although 3D RI tomograms provide detailed morphological and biochemical information of cells, the classification of lymphocyte subtypes is difficult to achieve by simply imaging 3D RI tomograms⁵. To systematically and quantitatively exploit the measured 3D RI tomograms for the cell type classification, we utilized a machine learning algorithm. Recently, several works have been reported in which quantitative phase images of cells were analyzed with various machine learning algorithms³³, including the detection of microorganisms³⁴, classification of bacterial genus^{35,36}, rapid and label-free detection of anthrax spores³⁷, automated analysis of sperm cells³⁸, analysis of cancer cells^{39,40}, and detection of macrophage activation⁴¹.

This protocol provides detailed steps to perform label-free identification of lymphocyte types at the individual cell level using 3D QPI and machine learning. This includes: 1) lymphocyte isolation from mouse blood, 2) lymphocyte sorting via flow cytometry, 3) 3D QPI, 4) quantitative feature extraction from 3D RI tomograms, and 5) supervised learning for identifying lymphocyte types.

PROTOCOL:

Animal care and experimental procedures were performed under the approval of the Institutional Animal Care and Use Committee of KAIST (KA2010-21, KA2014-01, and KA2015-03). All the experiments in this study were carried out in accordance with the approved guidelines.

1. Lymphocyte Isolation from Mouse Blood

1.1. Once a C57BL/6J mouse is euthanized via CO₂ inhalation, insert a 26-G needle into the mouse heart and collect 0.3 mL of blood. Directly put blood into a tube with 100 U/mL heparin solution diluted with 1 mL of phosphate-buffered saline (PBS).

NOTE: Alternatively, lymphocytes from the spleen can be isolated.

1.2. Centrifuge the tube at 400 x g for 5 min at 4 °C.

1.3. Add 0.5 mL of ammonium-chloride-potassium lysing buffer to the tube and gently invert it a few times to mix the solution.

1.4. Incubate the tube at room temperature (RT) for 5 min.

1.5. Wash the cells by adding 4.5 mL of PBS and centrifuging at 400 x g for 5 min at 4 °C, twice.

1.6. Remove the supernatant and resuspend the cell pellet in 100 µL of fresh RPMI-1640 medium with 10% fetal bovine serum (FBS).

1.7. Add 0.1 µg of CD16/32 (2.4G2) antibody to the tube for blocking.

1.8. Keep the tube on ice.

2. Flow Cytometry and Sorting of Lymphocyte Subtypes

Note: Sorting lymphocytes depending on cell type is essential for establishing the ground-truth (*i.e.*, correct) cell type labels to train and test a cell type classifier in supervised learning. Flow cytometry, a gold standard method, is used to identify and separate lymphocytes⁴².

2.1. Make a mixture of surface marker staining antibodies in 100 μ L of fresh RPMI-1640 medium [with 10% FBS, 0.1 μ g of CD3e (17A2), CD8a (53-6.7), CD19 (1D3), CD45R (B220, RA3-6B2), and NK1.1 (PK136)] and 0.25 μ g of CD4 (GK1.5) antibodies to target B, CD4⁺ T, and CD8⁺ T lymphocytes.

2.2. Add 100 μ L of the antibody mixture to the cell suspension (obtained in step 1.8).

2.3. Incubate for 25 min on ice.

2.4. Wash the cells by adding 5 mL of PBS and centrifuging at 400 x g for 5 min at 4 °C, twice.

2.5. Resuspend the cell pellet in 5 mL of fresh RPMI-1640 medium with 10% FBS and 2.5 μ g of DAPI (4,6-diamidino-2-phenylindole).

2.6. Collect each lymphocyte type separately with flow cytometry using the fluorescence levels of the markers described above. Simultaneously exclude dead cells using the DAPI signals.

Note: Detailed protocols regarding flow cytometry-based cell sorting have been described previously⁴².

3. 3D Quantitative Phase Imaging

3.1. Keep the sorted lymphocytes on ice throughout the imaging procedures, which should be completed within 5 h (since lymphocyte isolation from the mouse) to avoid cell damage and biochemical alterations.

3.2. Select a sorted cell type (among B, CD4⁺ T, and CD8⁺ T lymphocytes) and dilute the sample (obtained in step 2.6) to 180 cells/ μ L for optimal imaging condition (*i.e.*, one cell per single field-of-view).

3.3. Load 120 μ L of the diluted sample into an imaging chamber by slow injection. Thoroughly check on the presence of bubbles in the imaging chamber with the sample. If there are bubbles, carefully remove them, as they will compromise the quality of the measurements.

3.4. Acquire 3D RI tomograms using a commercial 3D quantitative phase microscope, or holotomography, and its imaging software.

Note: Detailed information about the experimental setup can be found in the original

manuscript⁵.

3.4.1. Place a drop of distilled water on top of the objective lens of the microscope.

3.4.2. Place the imaging chamber with the sample on the translation stage of the microscope and adjust its location so that the sample aligns with the objective lens.

3.4.3. Adjust the axial positions of the objective and condenser lenses by clicking **Focus** and **Surface**, respectively, on the “Calibration” tab of the “Microscope” perspective of the imaging software.

3.4.4. Align the objective and condenser lenses by clicking **Auto Mode**. Alternatively, use **Scanning Mode** and manually adjust the lenses so that the illumination patterns are localized at the central region of the field-of-view.

3.4.5. Return to **Normal Mode** and adjust the translation stage to locate a cell in the field-of-view.

3.4.6. Find the focal plane by adjusting the axial position of the objective lens. Perfect focusing makes the sample boundary visualized in the screen almost invisible.

3.4.7. Adjust the translation stage to find a location without a cell.

3.4.8. Click **Calibrate** to measure multiple 2D holograms with varying illumination angles.

3.4.9. Adjust the translation stage to locate a cell at the center of the field-of-view.

3.4.10. Move to the “Acquisition” tab and click **3D Snapshot** to measure the holograms of the cell with the identical illumination angles as done in step 3.4.8.

3.4.11. When the acquired data is presented on the “Data Management” panel, right-click on the acquired data and click **Process** to reconstruct a 3D RI tomogram from the holograms measured in steps 3.4.8 and 3.4.10, using the diffraction tomography algorithm^{9,10} implemented in the imaging software.

3.4.12. Repeat steps 3.4.5-3.4.11 to measure more than 100 cells to ensure statistical power for machine learning.

3.5. Repeat steps 3.2-3.4 to measure 3D RI tomograms of all lymphocyte subtypes.

4. Quantitative Morphological and Biochemical Feature Extraction from 3D RI Tomograms

4.1. Place all the tomographic data measured above in a single folder. Split the cell types in the subfolders of this folder. Prepare each tomogram to be a single *.mat* file.

221 4.2. Open **Supplementary File 1** (written for an image processing software).

222
223 4.3. Edit line 14 to designate the tomogram folder prepared in step 4.1.

224
225 4.4. Edit line 15 to designate a folder to save the extracted feature data.

226
227 4.5. Optionally, edit line 17 to adjust the RI threshold parameters for feature extraction. The
228 default option is 20 RI thresholds from 1.340-1.378, with an increment of 0.002 as described
229 previously⁵.

230
231 4.6. Execute the code. For every tomogram in the dataset, the code calculates five features:
232 surface area (SA), cellular volume (CV), sphericity (SI), protein density (PD), and dry mass (DM),
233 per RI threshold. The detailed algorithms for feature extraction are described elsewhere⁵.

234
235 4.7. In order to monitor the feature extraction, during the execution check on the screen
236 visualizing RI threshold-based cell segmentation.

237
238 4.8. Check on the extracted feature data, as *.mat* file per tomogram, saved in the folder
239 designated in step 4.4.

240 241 **5. Supervised Learning and Identification**

242
243 5.1. Randomly split the feature data obtained in step 4.8 to training (70%) and test (30%) sets
244 with separate folders.

245
246 5.2. Open **Supplementary File 2** (written for an image processing software).

247
248 5.3. Edit line 14 to designate the training set prepared in step 5.1.

249
250 5.4. Edit line 16 to designate a folder to save the trained classifier.

251
252 5.5. Edit line 17 to set a file name for the classifier.

253
254 5.6. Optionally, edit line 19 to select the features for training. The default option, as specified
255 previously⁵, was used to obtain the representative results below.

256
257 5.7. Execute the code. Using the selected features of the training set, the code trains a classifier
258 with the *k*-nearest neighbor algorithm (*k*-NN; *k* = 4) and then saves the classifier (as named in
259 step 5.5) in the folder designated in step 5.4.

260
261 5.8. Check on the screen visualizing the classifier performance and the cross-validation accuracy.

262
263 5.9. Optionally, train multiple classifiers with different feature combinations by repeating steps
264 5.5-5.7. Then choose the classifier with the highest cross-validation accuracy.

265
266 5.10. Open **Supplementary File 3** (written for an image processing software).

267
268 5.11. Edit lines 14-15 to designate the trained classifier to be tested.

269
270 5.12. Edit line 17 to designate the test set prepared in step 5.1.

271
272 5.13. Execute the code. The classifier described above identifies the cell types of the individual
273 lymphocytes in the test set.

274
275 5.14. Check on the screen visualizing the identification performance and the test accuracy.

276 277 **REPRESENTATIVE RESULTS:**

278 **Figure 1** shows the schematic process of the entire protocol. Using the procedure presented here,
279 we isolated B (n = 149), CD4+ T (n = 95), and CD8+ T (n = 112) lymphocytes. To obtain phase and
280 amplitude information at various angles of illumination, multiple 2D holograms of each
281 lymphocyte were measured by changing the angle of illumination (from -60° to 60°). Typically, 50
282 holograms can be used to reconstruct a 3D RI tomogram, but the number of 2D holograms can
283 be adjusted considering the imaging speed and quality. Amplitude and phase information of the
284 measured holograms are retrieved using a field retrieval algorithm based on Fourier
285 transform^{43,44}. The 3D RI tomogram of each lymphocyte was reconstructed from multiple 2D
286 retrieved phase and amplitude information at various angles of illumination using optical
287 diffraction tomography algorithm. Details of image process and 3D RI tomogram reconstruction
288 method can be found elsewhere^{21,45}.

289
290 **Figures 2A-2C** shows representative 3D rendered RI tomograms of B, CD4+ T, and CD8+ T
291 lymphocytes by allocating different color schemes according to RI values via the imaging
292 software. From the RI values, quantitative morphological (SA, CV, and SI) and biochemical (PD
293 and DM) features were calculated (**Figures 2A-2C**). This result clearly demonstrates that 3D RI
294 distribution enables quantitative analysis of morphological as well as biochemical information of
295 lymphocytes.

296
297 Supervised machine learning was exploited to identify lymphocyte types at a single-cell level. The
298 measured 3D RI tomograms were randomly split into 70% and 30% of training (B: 104, CD4+ T:
299 66, and CD8+ T: 77) and test (B: 45, CD4+ T: 29, and CD8+ T: 35) datasets, respectively. We
300 optimized the classifiers to maximally utilize the cell-type-specific fingerprints encoded in the
301 feature space. The total accuracy, sensitivity (true positive), and specificity (true negative) were
302 calculated by comparing the classifier-predicted results and ground-truth cell types.

303
304 In order to demonstrate proof-of-concept of the proposed protocol, we performed supervised
305 machine learning on three different cases: binary classification of (i) B and T lymphocytes and (ii)
306 two T lymphocyte subtypes (CD4+ and CD8+), and (iii) multiclass classification of all lymphocyte
307 types.
308

Figure 3 shows identification performance of optimized classifiers for training and test stages. The accuracy of the T and B lymphocyte classification was 93.15% and 89.81% for the training and test cases, respectively. The CD4+ and CD8+ T lymphocytes were statistically classified, and the accuracy was 87.41% and 84.38% for the training and test sets, respectively. Lastly, the accuracy of the multiclass cell type classifier was 80.65% and 75.93% for the training and test stages, respectively.

FIGURE AND TABLE LEGENDS:

Figure 1: Schematic diagrams of the label-free identification of lymphocyte types exploiting 3D quantitative phase imaging and machine learning.

Figure 2: Representative 3D rendered RI tomograms of each lymphocyte cell type with quantitative morphological and biochemical features. (A) B cell, (B) CD4+ T cell, and (C) CD8+ T cell. Scale bar = 2 μm . SA, surface area; CV, cellular volume; SI, sphericity; PD, protein density; DM, dry mass. This figure is modified with permission⁵.

Figure 3: Identification of individual lymphocyte types via supervised machine learning (A) binary classification of B and T cells, (B) binary classification of CD4+ and CD8+ T cells, and (C) multiclass classification of all three lymphocyte cell types; for both training and test sets. Note the small difference between the training and test cases, suggesting nice generalization of the established classifiers. The numbers below the names of each cell type indicate the number of cells used. This figure is modified with permission⁵.

Supplementary File 1: Feature extraction code. Extracting features (SA, CV, SI, PD, and DM) after RI threshold-based segmentation of each tomogram. Implemented in an image processing software.

Supplementary File 2: Training code. Training a k -NN classifier training based on selected features. Implemented in an image processing software.

Supplementary File 3: Testing code. Testing a trained k -NN classifier for a new dataset (*i.e.*, test set). Implemented in an image processing software.

DISCUSSION:

We present a protocol that enables the label-free identification of lymphocyte types exploiting 3D quantitative phase imaging and machine learning. Critical steps of this protocol are quantitative phase imaging and feature selection. For the optimal holographic imaging, the density of cells should be controlled as described above. Mechanical stability of the cells is also important to obtain a precise 3D RI distribution because floating or vibrational cellular motions will disturb hologram measurements upon illumination angle changes. We, therefore waited several minutes until the sample became stable and static in the imaging chamber before measuring holograms. Lastly, bubbles inside the imaging chamber are problematic when measuring holograms due to RI differences between air and the sample; thus, the sample should be carefully loaded to the imaging chamber.

Feature extraction and selection help determine the identification performance of the classifier. We calculated 5 quantitative morphological (CV, SA, SI) and biochemical (PD, DM) features from 3D RI distribution at 20 different RI threshold values; thus, we extracted a total of 100 features. We exhaustively searched optimal feature and classifier combinations, which show that the best cross-validation accuracy was selected. We tested 6 different machine learning algorithms, including k -NN ($k = 4$ and $k = 6$), linear discrimination analysis, quadratic discrimination analysis, naïve Bayes, and decision tree, and we found that k -NN ($k = 4$) showed the best identification performance. However, there is a chance to improve identification accuracy using other machine learning methods, including support vector machine and neuronal networks.

This protocol measures intrinsic optical properties via 3D quantitative phase imaging in order to identify lymphocyte types; thus, it does not require a labeling process based on antigen-antibody reactions used in fluorescence or magnetic bead-based cell-sorting techniques, which have risks of altering cellular function by modifying membrane protein structures. Moreover, the present method measures 3D RI distribution and provides 3D morphological and biochemical information about the cell, which cannot be obtained by a single-shot holography method⁴⁶; therefore, the identification performance of the protocol is more accurate due to high-dimensional information.

A minor limitation of this protocol is the manual adjustment of the sample stage and required labeling process for supervised machine learning. We searched a lymphocyte by adjusting the manual translational stage and measured holograms, which are the most time-consuming steps. This limitation would be improved by employing an automated motorized stage or microfluidic channel devices. Regarding supervised learning, the known lymphocyte types are required to establish the optimal classifier; thus, we had to first isolate and identify lymphocyte cell types based on the antigen-antibody-based sorting technique. Nonetheless, this protocol still uses the intrinsic optical contrast of lymphocytes, and the labeling agents used to specify antibodies have negligible effects on the measured 3D RI signal. Therefore, the established classifier may be used for identifying lymphocytes in a label-free manner.

Although this protocol mainly utilizes phenotypes of lymphocytes by measuring 3D RI tomograms of individual cells, these 3D RI data can also be used in combination with other modalities addressing genotypes or proteomic information for better classification of subtypes. Recently, correlative microscopy techniques combining fluorescence imaging and QPI have been introduced⁴⁷⁻⁴⁹. The approach presented in this protocol can also be extended to these correlative imaging methods.

Label-free identification of lymphocyte types can be applied to studying pathophysiology or diagnosing disease by detecting abnormal lymphocytes or ratios among lymphocyte types. Furthermore, this protocol can be applied to whole blood analysis by identifying various cells including red blood cells, platelets, and white blood cells.

ACKNOWLEDGMENTS:

This work was supported by the KAIST BK21+ Program, Tomocube, Inc., and the National

Research Foundation of Korea (2015R1A3A2066550, 2017M3C1A3013923, 2014K1A3A1A09063027). Y. Jo acknowledges support from the KAIST Presidential Fellowship and Asan Foundation Biomedical Science Scholarship.

DISCLOSURES:

Prof. Y. Park, Y. Jo, Y. S. Kim, and S. Lee have financial interests in Tomocube, Inc., a company that commercializes optical diffraction tomography and quantitative phase imaging instruments and is one of the sponsors of the work.

REFERENCES:

- 1 Alizadeh, A. A., *et al.* Distinct types of diffuse large B-cell lymphoma identified by gene expression profiling. *Nature*. **403** (6769), 503 (2000).
- 2 Von Boehmer, H., Melchers, F. Checkpoints in lymphocyte development and autoimmune disease. *Nature Immunology*. **11** (1), 14 (2010).
- 3 Sáez-Cirión, A., *et al.* HIV controllers exhibit potent CD8 T cell capacity to suppress HIV infection ex vivo and peculiar cytotoxic T lymphocyte activation phenotype. *Proceedings of the National Academy of Sciences*. **104** (16), 6776-6781 (2007).
- 4 Fischer, K., *et al.* Isolation and characterization of human antigen-specific TCR $\alpha\beta$ + CD4-CD8-double-negative regulatory T cells. *Blood*. **105** (7), 2828-2835 (2005).
- 5 Yoon, J., *et al.* Identification of non-activated lymphocytes using three-dimensional refractive index tomography and machine learning. *Scientific Reports*. **7** (1), 6654 (2017).
- 6 Popescu, G. Quantitative phase imaging of cells and tissues. (McGraw Hill Professional, 2011).
- 7 Lee, K. *et al.* Quantitative phase imaging techniques for the study of cell pathophysiology: from principles to applications. *Sensors*. **13** (4), 4170-4191 (2013).
- 8 Kim, D., *et al.* Refractive index as an intrinsic imaging contrast for 3-D label-free live cell imaging. *bioRxiv*. 106328 (2017).
- 9 Kim, K., *et al.* Optical diffraction tomography techniques for the study of cell pathophysiology. *Journal of Biomedical Photonics & Engineering*. **2** (2), (2016).
- 10 Wolf, E. Three-dimensional structure determination of semi-transparent objects from holographic data. *Optics Communications*. **1** (4), 153-156 (1969).
- 11 Kuś, A., Dudek, M., Kemper, B., Kujawińska, M., Vollmer, A. *SPIE - the international society for optics and photonics*. 8.
- 12 Kim, T., *et al.* White-light diffraction tomography of unlabelled live cells. *Nature Photonics*. **8** (3), 256 (2014).
- 13 Simon, B., *et al.* Tomographic diffractive microscopy with isotropic resolution. *Optica*. **4** (4), 460-463 (2017).
- 14 Kim, Y., *et al.* Profiling individual human red blood cells using common-path diffraction optical tomography. *Scientific Reports*. **4**, (2014).
- 15 Park, H., *et al.* Measuring cell surface area and deformability of individual human red blood cells over blood storage using quantitative phase imaging. *Scientific Reports*. **6**, (2016).
- 16 Lee, S., *et al.* Refractive index tomograms and dynamic membrane fluctuations of red blood cells from patients with diabetes mellitus. *Scientific Reports*. **7**, (2017).

- 441 17 Merola, F., *et al.* Tomographic flow cytometry by digital holography. *Light-Science &*
442 *Applications*. **6**, (2017).
- 443 18 Park, Y., *et al.* Refractive index maps and membrane dynamics of human red blood cells
444 parasitized by Plasmodium falciparum. *Proceedings of the National Academy of Sciences*.
445 **105** (37), 13730-13735 (2008).
- 446 19 Park, H., *et al.* Characterizations of individual mouse red blood cells parasitized by Babesia
447 microti using 3-D holographic microscopy. *Scientific Reports*. **5**, 10827 (2015).
- 448 20 Chandramohanadas, R., *et al.* Biophysics of malarial parasite exit from infected
449 erythrocytes. *Public Library of Science ONE*. **6** (6), e20869 (2011).
- 450 21 Yoon, J., *et al.* Label-free characterization of white blood cells by measuring 3D refractive
451 index maps. *Biomedical Optics Express*. **6** (10), 3865-3875 (2015).
- 452 22 Kim, K., *et al.* Three-dimensional label-free imaging and quantification of lipid droplets in
453 live hepatocytes. *Scientific Reports*. **6**, 36815 (2016).
- 454 23 Kim, D., *et al.* Label-free high-resolution 3-D imaging of gold nanoparticles inside live cells
455 using optical diffraction tomography. *Methods*. (2017).
- 456 24 Lenz, P., *et al.* Multimodal Quantitative Phase Imaging with Digital Holographic
457 Microscopy Accurately Assesses Intestinal Inflammation and Epithelial Wound Healing.
458 *Journal of Visualized Experiments*. (115), (2016).
- 459 25 Huang, J., Guo, P., Moses, M. A. A Time-lapse, Label-free, Quantitative Phase Imaging
460 Study of Dormant and Active Human Cancer Cells. *Journal of Visualized Experiments*.
461 (132), (2018).
- 462 26 Yang, S. A., Yoon, J., Kim, K., Park, Y. Measurements of morphological and biochemical
463 alterations in individual neuron cells associated with early neurotoxic effects in
464 Parkinson's disease. *Cytometry Part A*. **91** (5), 510-518 (2017).
- 465 27 Cotte, Y., *et al.* Marker-free phase nanoscopy. *Nature Photonics*. **7** (2), 113-117 (2013).
- 466 28 Nguyen, T. H., Kandel, M. E., Rubessa, M., Wheeler, M. B. & Popescu, G. Gradient light
467 interference microscopy for 3D imaging of unlabeled specimens. *Nature Communications*.
468 **8** (1), 210 (2017).
- 469 29 Kwon, S. *et al.* Mitochondria-targeting indolizino [3, 2-c] quinolines as novel class of
470 photosensitizers for photodynamic anticancer activity. *European Journal of Medicinal*
471 *Chemistry*. **148**, 116-127 (2018).
- 472 30 Bennet, M., Gur, D., Yoon, J., Park, Y., Faivre, D. A Bacteria-Based Remotely Tunable
473 Photonic Device. *Advanced Optical Materials*. (2016).
- 474 31 Kim, T. I., *et al.* Antibacterial Activities of Graphene Oxide–Molybdenum Disulfide
475 Nanocomposite Films. *ACS Applied Materials & Interfaces*. **9** (9), 7908-7917 (2017).
- 476 32 Bedrossian, M., Barr, C., Lindensmith, C. A., Nealson, K., Nadeau, J. L. Quantifying
477 Microorganisms at Low Concentrations Using Digital Holographic Microscopy (DHM).
478 *Journal of Visualized Experiments*. (129), (2017).
- 479 33 Jo, Y., *et al.* Quantitative Phase Imaging and Artificial Intelligence: A Review. *arXiv preprint*
480 *arXiv:1806.03982*. (2018).
- 481 34 Javidi, B., Moon, I., Yeom, S., Carapezza, E. Three-dimensional imaging and recognition of
482 microorganism using single-exposure on-line (SEOL) digital holography. *Optics Express*. **13**
483 (12), 4492-4506 (2005).
- 484 35 Jo, Y., *et al.* Label-free identification of individual bacteria using Fourier transform light

scattering. *Optics Express*. **23** (12), 15792-15805 (2015).

36 Jo, Y., *et al.* Angle-resolved light scattering of individual rod-shaped bacteria based on Fourier transform light scattering. *Scientific Reports*. **4**, 5090 (2014).

37 Jo, Y., *et al.* Holographic deep learning for rapid optical screening of anthrax spores. *Science Advances*. **3** (8), e1700606 (2017).

38 Mirsky, S. K., Barnea, I., Levi, M., Greenspan, H., Shaked, N. T. Automated analysis of individual sperm cells using stain-free interferometric phase microscopy and machine learning. *Cytometry Part A*. **91** (9), 893-900 (2017).

39 Roitshtain, D., *et al.* Quantitative phase microscopy spatial signatures of cancer cells. *Cytometry Part A*. **91** (5), 482-493 (2017).

40 Lam, V. K., Nguyen, T. C., Chung, B. M., Nehmetallah, G., Raub, C. B. Quantitative assessment of cancer cell morphology and motility using telecentric digital holographic microscopy and machine learning. *Cytometry Part A*. (2017).

41 Pavillon, N., Hobro, A. J., Akira, S., Smith, N. I. Noninvasive detection of macrophage activation with single-cell resolution through machine learning. *Proceedings of the National Academy of Sciences*. 201711872 (2018).

42 Basu, S., Campbell, H. M., Dittel, B. N., Ray, A. Purification of Specific Cell Population by Fluorescence Activated Cell Sorting (FACS). *Journal of Visualized Experiments*. (41), e1546 (2010).

43 Takeda, M., Ina, H., Kobayashi, S. Fourier-transform method of fringe-pattern analysis for computer-based topography and interferometry. *Journal of the Optical Society of America*. **72** (1), 156-160 (1982).

44 Debnath, S. K., Park, Y. Real-time quantitative phase imaging with a spatial phase-shifting algorithm. *Optics Letters*. **36** (23), 4677-4679 (2011).

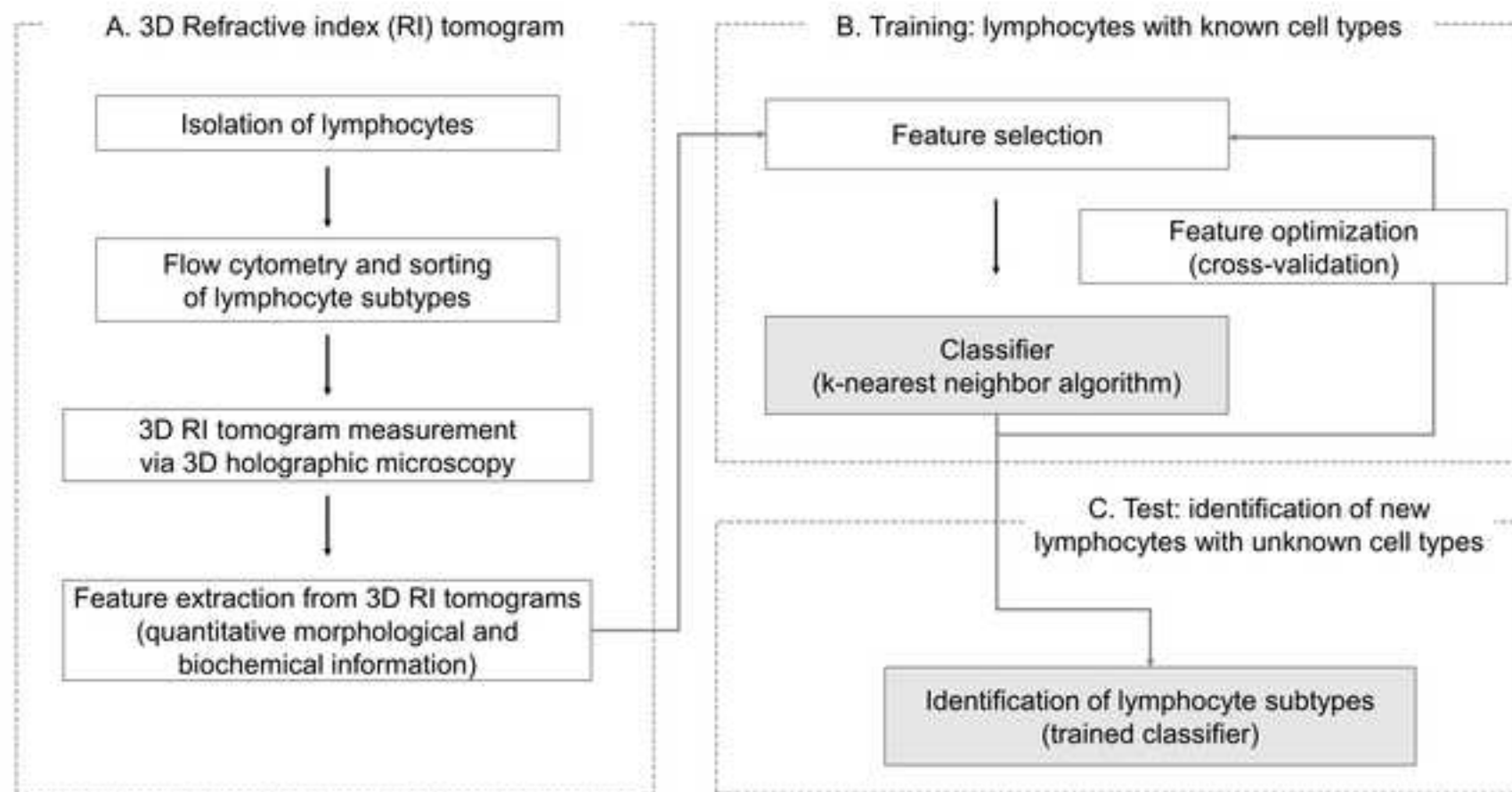
45 Kim, K., *et al.* High-resolution three-dimensional imaging of red blood cells parasitized by *Plasmodium falciparum* and in situ hemozoin crystals using optical diffraction tomography. *Journal of Biomedical Optics*. **19** (1), 011005 (2013).

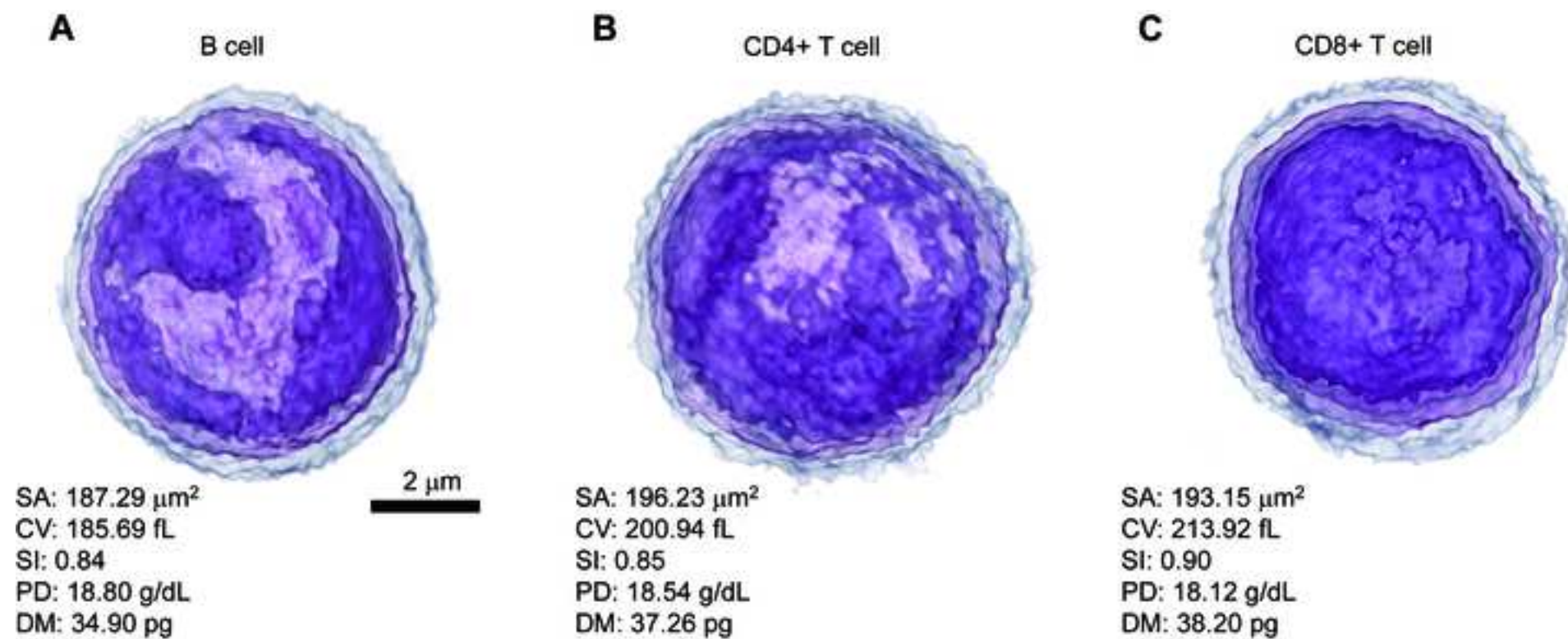
46 Vercruysse, D., *et al.* Three-part differential of unlabeled leukocytes with a compact lens-free imaging flow cytometer. *Lab on a Chip*. **15** (4), 1123-1132 (2015).

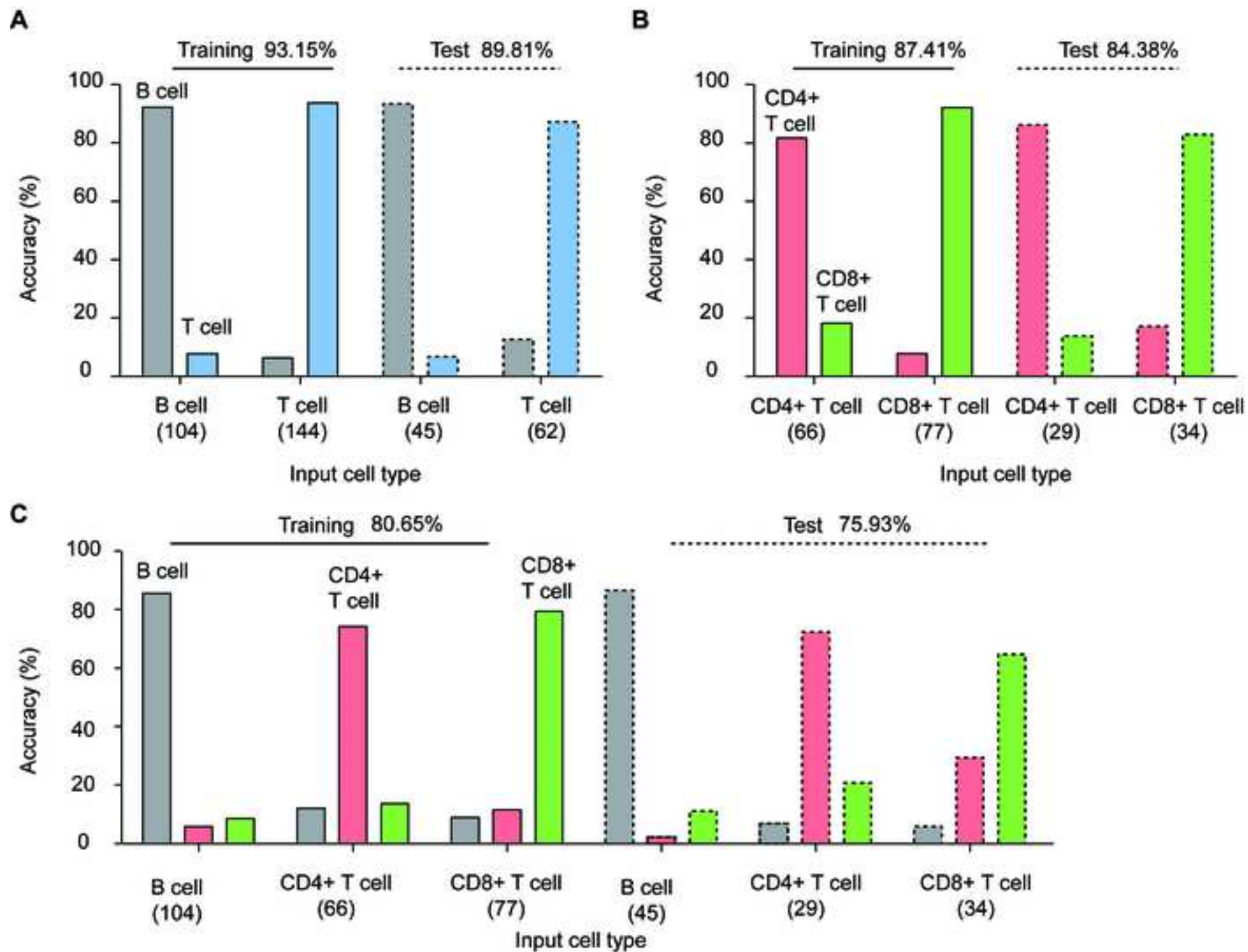
47 Kim, K., *et al.* Correlative three-dimensional fluorescence and refractive index tomography: bridging the gap between molecular specificity and quantitative bioimaging. *Biomedical Optics Express*. **8** (12), 5688-5697 (2017).

48 Shin, S., Kim, D., Kim, K., Park, Y. Super-resolution three-dimensional fluorescence and optical diffraction tomography of live cells using structured illumination generated by a digital micromirror device. *arXiv preprint arXiv:1801.00854*. (2018).

49 Chowdhury, S., Eldridge, W. J., Wax, A., Izatt, J. A. Structured illumination multimodal 3D-resolved quantitative phase and fluorescence sub-diffraction microscopy. *Biomedical Optics Express*. **8** (5), 2496-2518 (2017).







Name of Material/Equipment	Company
Mouse	Daehan Biolink
Falcon conical centrifuge tube	ThermoFisher Scientific
Phosphate-buffered saline	Sigma-Aldrich
Ammonium-chloride-potassium lysing buffer	ThermoFisher Scientific
RPMI-1640 medium	Sigma-Aldrich
Fetal bovine serum	ThermoFisher Scientific
Antibody	BD Biosciences
Antibody	BD Biosciences
Antibody	Biolegnd
Antibody	BD Biosciences
Antibody	BD Biosciences
Antibody	BD Biosciences
Antibody	eBioscience
DAPI	Roche
Flow cytometry	BD Biosciences
Imaging chamber	Tomocube, Inc.
Holotomography	Tomocube, Inc.
Holotomography imaging software	Tomocube, Inc.
Image professing software	MathWorks

Catalog Number	Comments/Description
C57BL/6J mice	gender and age-matched, 6 – 8 weeks
14-959-53A	15 mL
806544-500ML	
A1049201	
R8758	
10438018	
553140 (RRID:AB_394655)	CD16/32 (clone 2.4G2)
555275 (RRID:AB_395699)	CD3 ϵ (clone 17A2)
100734 (RRID:AB_2075238)	CD8 α (clone 53-6.7)
557655 (RRID:AB_396770)	CD19 (clone 1D3)
557683 (RRID:AB_396793)	CD45R/B220 (clone RA3-6B2)
552878 (RRID:AB_394507)	NK1.1 (clone PK136)
11-0041-85 (RRID:AB_464893)	CD4 (clone GK1.5)
10236276001	4,6-diamidino-2-phenylindole
Aria II or III	
TomoDish	
HT-1H	
TomoStudio	
Matlab R2017b	

ARTICLE AND VIDEO LICENSE AGREEMENT - UK

Title of Article:	Label-free identification of lymphocyte subtypes using 3D quantitative phase imaging and machine learning
Author(s):	Jonghee Yoon, YoungJu Jo, Young Seo Kim, Yeongjin Yu, Jiyeon Park, Sumin Lee, Wei Sun Park, and YongKeun Park

Item 1: The Author elects to have the Materials be made available (as described at <http://www.jove.com/publish>) via:

☒ Standard Access

☐ Open Access

Item 2: Please select one of the following items:

☒ The Author is **NOT** a United States government employee.

☐ The Author is a United States government employee and the Materials were prepared in the course of his or her duties as a United States government employee.

☐ The Author is a United States government employee but the Materials were NOT prepared in the course of his or her duties as a United States government employee.

ARTICLE AND VIDEO LICENSE AGREEMENT

1. **Defined Terms.** As used in this Article and Video License Agreement, the following terms shall have the following meanings: "**Agreement**" means this Article and Video License Agreement; "**Article**" means the article specified on the last page of this Agreement, including any associated materials such as texts, figures, tables, artwork, abstracts, or summaries contained therein; "**Author**" means the author who is a signatory to this Agreement; "**Collective Work**" means a work, such as a periodical issue, anthology or encyclopedia, in which the Materials in their entirety in unmodified form, along with a number of other contributions, constituting separate and independent works in themselves, are assembled into a collective whole; "**CRC License**" means the Creative Commons Attribution 3.0 Agreement (also known as CC-BY), the terms and conditions of which can be found at: <http://creativecommons.org/licenses/by/3.0/us/legalcode>; "**Derivative Work**" means a work based upon the Materials or upon the Materials and other pre-existing works, such as a translation, musical arrangement, dramatization, fictionalization, motion picture version, sound recording, art reproduction, abridgment, condensation, or any other form in which the Materials may be recast, transformed, or adapted; "**Institution**" means the institution, listed on the last page of this Agreement, by which the Author was employed at the time of the creation of the Materials; "**JoVE**" means MyJoVE Corporation, a Massachusetts corporation and the publisher of The Journal of Visualized Experiments; "**Materials**" means the Article and / or the Video; "**Parties**" means the Author and JoVE; "**Video**" means any video(s) made by the Author, alone or in conjunction with any other parties, or by JoVE or its affiliates or agents, individually or in collaboration with the Author or any other parties, incorporating all or any portion

of the Article, and in which the Author may or may not appear.

2. **Background.** The Author, who is the author of the Article, in order to ensure the dissemination and protection of the Article, desires to have the JoVE publish the Article and create and transmit videos based on the Article. In furtherance of such goals, the Parties desire to memorialize in this Agreement the respective rights of each Party in and to the Article and the Video.

3. **Grant of Rights in Article.** In consideration of JoVE agreeing to publish the Article, the Author hereby grants to JoVE, subject to **Sections 4 and 7** below, the exclusive, royalty-free, perpetual (for the full term of copyright in the Article, including any extensions thereto) license (a) to publish, reproduce, distribute, display and store the Article in all forms, formats and media whether now known or hereafter developed (including without limitation in print, digital and electronic form) throughout the world, (b) to translate the Article into other languages, create adaptations, summaries or extracts of the Article or other Derivative Works (including, without limitation, the Video) or Collective Works based on all or any portion of the Article and exercise all of the rights set forth in (a) above in such translations, adaptations, summaries, extracts, Derivative Works or Collective Works and (c) to license others to do any or all of the above. The foregoing rights may be exercised in all media and formats, whether now known or hereafter devised, and include the right to make such modifications as are technically necessary to exercise the rights in other media and formats. If the "Open Access" box has been checked in **Item 1** above, JoVE and the Author hereby grant to the public all such rights in the Article as provided in, but subject to all limitations and requirements set forth in, the CRC License.

4. **Retention of Rights in Article.** Notwithstanding the exclusive license granted to JoVE in **Section 3** above, the Author shall, with respect to the Article, retain the non-exclusive right to use all or part of the Article for the non-commercial purpose of giving lectures, presentations or teaching classes, and to post a copy of the Article on the Institution's website or the Author's personal website, in each case provided that a link to the Article on the JoVE website is provided and notice of JoVE's copyright in the Article is included. All non-copyright intellectual property rights in and to the Article, such as patent rights, shall remain with the Author.

5. **Grant of Rights in Video - Standard Access.** This **Section 5** applies if the "Standard Access" box has been checked in **Item 1** above or if no box has been checked in **Item 1** above. In consideration of JoVE agreeing to produce, display or otherwise assist with the Video, the Author hereby acknowledges and agrees that, subject to **Section 7** below, JoVE is and shall be the sole and exclusive owner of all rights of any nature, including, without limitation, all copyrights, in and to the Video. To the extent that, by law, the Author is deemed, now or at any time in the future, to have any rights of any nature in or to the Video, the Author hereby disclaims all such rights and transfers all such rights to JoVE.

6. **Grant of Rights in Video - Open Access.** This **Section 6** applies only if the "Open Access" box has been checked in **Item 1** above. In consideration of JoVE agreeing to produce, display or otherwise assist with the Video, the Author hereby grants to JoVE, subject to **Section 7** below, the exclusive, royalty-free, perpetual (for the full term of copyright in the Article, including any extensions thereto) license (a) to publish, reproduce, distribute, display and store the Video in all forms, formats and media whether now known or hereafter developed (including without limitation in print, digital and electronic form) throughout the world, (b) to translate the Video into other languages, create adaptations, summaries or extracts of the Video or other Derivative Works or Collective Works based on all or any portion of the Video and exercise all of the rights set forth in (a) above in such translations, adaptations, summaries, extracts, Derivative Works or Collective Works and (c) to license others to do any or all of the above. The foregoing rights may be exercised in all media and formats, whether now known or hereafter devised, and include the right to make such modifications as are technically necessary to exercise the rights in other media and formats.

7. **Government Employees.** If the Author is a United States government employee and the Article was prepared in the course of his or her duties as a United States government employee, as indicated in **Item 2** above, and any of the licenses or grants granted by the Author hereunder exceed the scope of the 17 U.S.C. 403, then the rights granted hereunder shall be limited to the maximum rights permitted under such statute. In such case, all provisions contained herein that are not in conflict with such statute shall remain in full force and effect, and all provisions contained herein that do so conflict shall be

deemed to be amended so as to provide to JoVE the maximum rights permissible within such statute.

8. **Protection of the work.** The Author(s) authorize JoVE to take steps in the Author(s) name and on their behalf if JoVE believes some third party could be infringing or might infringe the copyright of either the Author's Article and/or Video.

9. **Likeness, Privacy, Personality.** The Author hereby grants JoVE the right to use the Author's name, voice, likeness, picture, photograph, image, biography and performance in any way, commercial or otherwise, in connection with the Materials and the sale, promotion and distribution thereof. The Author hereby waives any and all rights he or she may have, relating to his or her appearance in the Video or otherwise relating to the Materials, under all applicable privacy, likeness, personality or similar laws.

10. **Author Warranties.** The Author represents and warrants that the Article is original, that it has not been published, that the copyright interest is owned by the Author (or, if more than one author is listed at the beginning of this Agreement, by such authors collectively) and has not been assigned, licensed, or otherwise transferred to any other party. The Author represents and warrants that the author(s) listed at the top of this Agreement are the only authors of the Materials. If more than one author is listed at the top of this Agreement and if any such author has not entered into a separate Article and Video License Agreement with JoVE relating to the Materials, the Author represents and warrants that the Author has been authorized by each of the other such authors to execute this Agreement on his or her behalf and to bind him or her with respect to the terms of this Agreement as if each of them had been a party hereto as an Author. The Author warrants that the use, reproduction, distribution, public or private performance or display, and/or modification of all or any portion of the Materials does not and will not violate, infringe and/or misappropriate the patent, trademark, intellectual property or other rights of any third party. The Author represents and warrants that it has and will continue to comply with all government, institutional and other regulations, including, without limitation all institutional, laboratory, hospital, ethical, human and animal treatment, privacy, and all other rules, regulations, laws, procedures or guidelines, applicable to the Materials, and that all research involving human and animal subjects has been approved by the Author's relevant institutional review board.

11. **JoVE Discretion.** If the Author requests the assistance of JoVE in producing the Video in the Author's facility, the Author shall ensure that the presence of JoVE employees, agents or independent contractors is in accordance with the relevant regulations of the Author's institution. If more than one author is listed at the beginning of this Agreement, JoVE may, in its sole discretion, elect not take any action with respect to the Article until such time as it has received complete, executed Article and Video License Agreements from each such author. JoVE reserves the right, in its absolute and sole

discretion and without giving any reason therefore, to accept or decline any work submitted to JoVE. JoVE and its employees, agents and independent contractors shall have full, unfettered access to the facilities of the Author or of the Author's institution as necessary to make the Video, whether actually published or not. JoVE has sole discretion as to the method of making and publishing the Materials, including, without limitation, to all decisions regarding editing, lighting, filming, timing of publication, if any, length, quality, content and the like.

12. **Indemnification.** The Author agrees to indemnify JoVE and/or its successors and assigns from and against any and all claims, costs, and expenses, including attorney's fees, arising out of any breach of any warranty or other representations contained herein. The Author further agrees to indemnify and hold harmless JoVE from and against any and all claims, costs, and expenses, including attorney's fees, resulting from the breach by the Author of any representation or warranty contained herein or from allegations or instances of violation of intellectual property rights, damage to the Author's or the Author's institution's facilities, fraud, libel, defamation, research, equipment, experiments, property damage, personal injury, violations of institutional, laboratory, hospital, ethical, human and animal treatment, privacy or other rules, regulations, laws, procedures or guidelines, liabilities and other losses or damages related in any way to the submission of work to JoVE, making of videos by JoVE, or publication in JoVE or elsewhere by JoVE. The Author shall be responsible for, and shall hold JoVE harmless from, damages caused by lack of sterilization, lack of cleanliness or by contamination due to the making of a video by JoVE its employees, agents or independent contractors. All sterilization, cleanliness or

decontamination procedures shall be solely the responsibility of the Author and shall be undertaken at the Author's expense. All indemnifications provided herein shall include JoVE's attorney's fees and costs related to said losses or damages. Such indemnification and holding harmless shall include such losses or damages incurred by, in connection with, acts or omissions of JoVE, its employees, agents or independent contractors.

13. **Fees.** To cover the cost incurred for publication, JoVE must receive payment before production and publication of the Materials. Payment is due in 21 days of invoice. Should the Materials not be published due to an editorial or production decision, these funds will be returned to the Author. Withdrawal by the Author of any submitted Materials after final peer review approval will result in a US\$1,200 fee to cover pre-production expenses incurred by JoVE. If payment is not received by the completion of filming, production and publication of the Materials will be suspended until payment is received.

14. **Transfer, Governing Law.** This Agreement may be assigned by JoVE and shall inure to the benefit of any of JoVE's successors and assignees. This Agreement shall be governed and construed by the internal laws of the Commonwealth of Massachusetts without giving effect to any conflict of law provision thereunder. This Agreement may be executed in counterparts, each of which shall be deemed an original, but all of which together shall be deemed to be one and the same agreement. A signed copy of this Agreement delivered by facsimile, e-mail or other means of electronic transmission shall be deemed to have the same legal effect as delivery of an original signed copy of this Agreement.

A signed copy of this document must be sent with all new submissions. Only one Agreement is required per submission.

CORRESPONDING AUTHOR

Name:	Jonghee Yoon	
Department:	Department of Physics	
Institution:	University of Cambridge	
Title:	Postdoctoral Research Associate	
Signature:	Jonghee Yoon	Date: 2018.07.18

Please submit a **signed and dated** copy of this license by one of the following three methods:

1. Upload an electronic version on the JoVE submission site
2. Fax the document to +1.866.381.2236
3. Mail the document to JoVE / Attn: JoVE Editorial / 1 Alewife Center #200 / Cambridge, MA 02140

Editorial comments:

1. The editor has formatted the manuscript to match the journal's style. Please retain the same.

[We thank the Editor for formmating our manuscript. We retained the style during revision.](#)

2. Please address all specific comments marked in the manuscript. Also, please reword the title better.

[As suggested, we addressed all specific comments marked in the manuscript by the Editor. Also, we modified the title.](#)

3. For the protocol section, please ensure that the "how" question is answered- How is this step performed?

[As suggested, we thoroughly revised the protocol section to provide detailed experimental steps answering the “how” questions.](#)

4. Please ensure that the highlighted portion of the protocol contains hard experimental steps, graphical user interface, button clicks on the software, knob turns etc. We cannot film calculation steps and steps which are abstract.

[As suggested, we also thoroughly revised the highlighted portion of the protocol with considerations about filming.](#)

6. Since one of the authors is from UK, please sign the UK ALA. Please ensure that the author is allowed to publish standard access.

[We attached the document in the revised submission.](#)

7. Please proofread the manuscript well before submission.

[As suggested, we proofread the manuscript multiple times to guarantee the manuscript quality.](#)

제 목 : RE: Permission inquiry for using figures in SciRep paper.

보내는사람 : Journalpermissions
받는사람 : "jh.yoon@kaist.ac.kr"
참조 : ReprintsWarehouse
보낸 날짜 : 2018-04-03 22:06:04

Dear Jonghee,

Thank you for your email, I can confirm that you do not need to obtain permission to reuse this content provided you clearly acknowledge the original source.

Kind Regards,

Claire Harper (née Smith)
Journal Permissions Manager

SpringerNature
The Campus, 4 Crinan Street, London N1 9XW, United Kingdom
T +44 (0) 207 014 4129

From: 윤종희 [<mailto:jh.yoon@kaist.ac.kr>]
Sent: 01 April 2018 18:08
To: ReprintsWarehouse
Subject: Permission inquiry for using figures in SciRep paper.

Dear Springer Nature Scientific Reports,

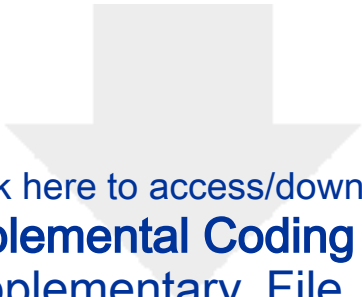
I'm the author of "Identification of non-activated lymphocytes using three-dimensional refractive index tomography and machine learning" published in Scientific Reports at 2017.

I ask permissions to use Figs 2.(D-F) and Figs4. (A-C) for the new article which will be submitted to Journal of Visualized Experiments (JoVE).

When I check the copyright of this paper, this paper permits unrestricted use with proper citation.
Then, could I use and modify the figures in this paper by proper citation? Or do I require permissions to reuse it?

If you need any further information, please let me know.

Best wishes,
Jonghee



Click here to access/download
Supplemental Coding Files
Supplementary_File_1.m





Click here to access/download
Supplemental Coding Files
Supplementary_File_2.m





Click here to access/download
Supplemental Coding Files
Supplementary_File_3.m

